

Oxygen Surface Diffusion and Surface Layer Thickness in Oxides Measured by ^{18}O -Exchange Reaction

Yasuro IKUMA and Wazo KOMATSU

Abstract

An oxygen isotope exchange reaction between ^{18}O oxygen gas and oxide powder (MgO, NiO, and Y_2O_3) was monitored with a microbalance. The weight change of the specimen was plotted as a function of the square root of time which resulted in a curve having two straight lines with a transition region between them. The first steep line was due to the oxygen exchange reaction within the surface layer and the less steep line was probably due to the oxygen lattice diffusion or grain boundary diffusion. From the first steep lines at various temperatures (300–900°C) the oxygen surface diffusion coefficients were calculated. The surface diffusion measured by the current method was diffusion through a surface layer rather than diffusion along surface. The oxygen surface diffusion coefficients of MgO and NiO are always several orders of magnitude lower than the surface diffusion coefficients reported in the literature. Two possible reasons to this discrepancy were discussed. From the weight gain at the intersection of the two lines, the surface layer thicknesses of these oxides have been estimated. The surface layer thicknesses were 0.3–4.6 nm and had a small positive temperature dependence. The surface layer thicknesses measured by the present method were in general smaller than those obtained by a kinetic method.

I. Introduction

It is well known that the surface diffusion coefficient and surface layer thickness* are some of the important parameters in understanding the kinetic processes of powder, such as sintering and solid state reactions. In the past, several methods have been used to determine these parameters related to the surface. The product of the surface diffusion coefficient and surface layer thickness appears in the kinetic equation of combined sintering and in the solution of differential equation of diffusion involving the surface diffusion. Therefore, the product can be obtained by studying the sintering¹⁾ or by the well-prepared diffusion experiment.²⁾ The limitation of these methods is that only the product of the quantities can be determined and the estimation of the individual quantity is not possible. Thermal grooving and scratch smoothing methods which are based on the theory developed by Mullins and others^{3)–6)} are other ways to determine the parameters related to the surface. In these methods the surface diffusion coefficients for single crystals, bicrystals and sintered body can be determined. However, no surface diffusion for powder can be studied. Furthermore, the estimation of surface layer thickness is not possible in these methods. Instead of measuring the surface layer thickness, it has been generally assumed that $\delta = \mathcal{Q}^{1/3}$, where δ is the surface layer thickness and \mathcal{Q} is the atomic (or ionic) volume of diffusing species.

* We define the thickness of surface layer to be the width of region where the diffusion is enhanced due to a disturbed structure.

Received Oct. 1, 1983

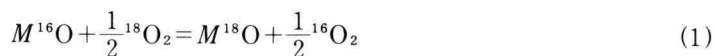
In our laboratory, the surface layer thickness of powder has been measured by making use of the solid state reactions between two kinds of powder and the reactions between solids and gases (kinetic method).⁷⁾⁻⁹⁾ Although the surface layer thickness can be estimated independently in this method, a disadvantage is that there are not always any appropriate solid reactions to be utilized in the measurement of surface layer thickness of all the oxides. Another important fact concerning the kinetic method is that the surface layer thickness is measured at a very special moment when the products are just formed. The product at this moment has generally a disturbed structure¹⁰⁾⁻¹²⁾ where the diffusion is expected to be enhanced. Consequently, the surface layer thickness measured by this method might be overestimated.

Recently the authors^{13),14)} have developed a new method in which the surface diffusion coefficient and the surface layer thickness can be measured concurrently and independently (isotope exchange method). In this method, we follow the oxygen isotope exchange reaction between $^{18}\text{O}_2$ gas and oxide powder by measuring the weight of the specimen. Since we can record the diffusion process continuously with a microbalance, we are able to gain important information which is sometimes not detected in the conventional diffusion experiment. From the measurement of weight gain both the surface diffusion coefficient and the surface layer thickness can be evaluated independently. In this paper the surface diffusion coefficients and surface layer thicknesses of some oxide powders (MgO, NiO and Y_2O_3) obtained by the isotope exchange method will be presented and compared with the values in the literature.

II. Experimental

2.1 Principle

The principle used in this study is as follows: when an oxide ($M^{16}\text{O}$, where M is a cation with an assumed valence of 2+) is heated in an oxygen atmosphere enriched with the isotope ^{18}O , an oxygen exchange reaction given by Eq. (1) takes place on the surface of oxide.



Then the oxygen (^{18}O) diffuses into the bulk. Due to the difference in atomic weight between ^{16}O and ^{18}O , the oxide receives weight gain. In order to follow the diffusion process, the weight gain was monitored continuously with a microbalance.

2.2 Specimens

Three oxides were selected for the diffusion study. They were MgO, NiO, and Y_2O_3 .

Nominally pure MgO* (Rare Metallic Co.) was annealed in a platinum crucible at the temperature of 1150°C and the oxygen pressure of 6.7×10^3 Pa for 3 hrs. The surface area

* After the annealing at 1150°C for 3 hrs the impurity content was measured by emission spectroscopy. The major impurities were Si (~200 ppm), Fe (~60 ppm), Mn (10-60 ppm), and P (10-60 ppm).

($18.35 \text{ m}^2/\text{g}$) of the specimen was determined by BET method. Assuming that the specimen consists of spherical powder, the average particle size of 46 nm was calculated from the BET surface area.

High purity (99.999%) NiO (Halewood Chemicals) was annealed in an $^{16}\text{O}_2$ atmosphere of $6.7 \times 10^3 \text{ Pa}$ at 800°C for 24 hrs. The sample was slightly ground in an agate mortar. The average particle diameter of the NiO powder measured by SEM was $0.29 \mu\text{m}$ which was in good agreement with that ($0.24 \mu\text{m}$) estimated from the BET area ($3.75 \text{ m}^2/\text{g}$). The diameter obtained from X-ray diffraction patterns of (101) and (033) planes was $0.06 \mu\text{m}$. Therefore, the particle of NiO was not a single grain but a well sintered particle consisting of about one hundred grains.

High purity Y_2O_3 (Rare Metallic Co., nominally 99.9%) was annealed at various temperatures to obtain specimens with different grain sizes. The particle sizes calculated from the BET surface area of specimens annealed at 750°C , 1000°C , and 1300°C were $0.099 \mu\text{m}$, $0.12 \mu\text{m}$, and $0.20 \mu\text{m}$, respectively.

2.3 Apparatus and Diffusion Annealing

The apparatus consisted of a reaction chamber shown in Fig. 1, a microbalance (Shimadzu RMB-50V), and a vacuum system with a mercury manometer. The volume of the gas phase was 1344 ml . The exchange reaction was carried out in the reaction chamber

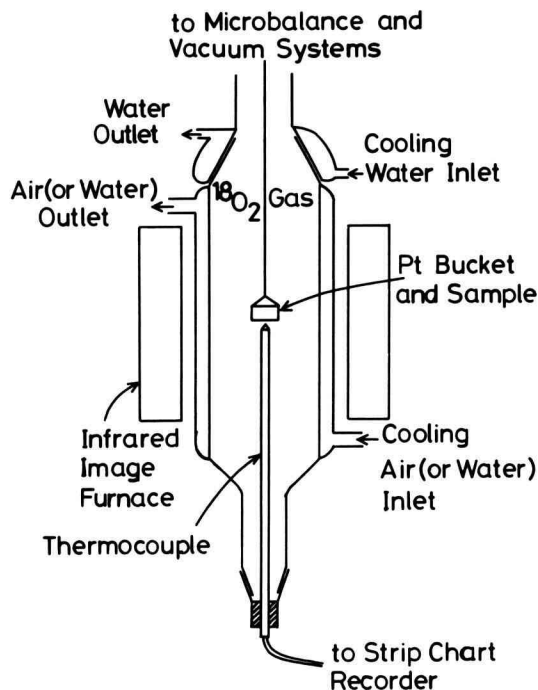


Fig. 1. Schematic of exchange reaction chamber.

made of quartz glass. The chamber was 40 mm in diameter and 260 mm long, and was equipped with a cooling jacket as shown in Fig. 1. The gap between two walls of the jacket was 2 mm through which cooling air (or water if the temperature of specimen was more than 700°C) passed with the flow rate of 3000 l/h (144 l/h for water). A platinum bucket (pure Pt or Pt+20% Rh) hanging on the microbalance with a thin Pt-wire was adjusted such that it was located at the center of the chamber. An infrared image furnace (Shinkuriko RHL-E45) was used to heat the sample in the Pt bucket. The minimum rate of weight change that could be detected with this microbalance was 0.01 mg/h. The temperature was measured with a Pt-Pt 13% Rh thermocouple located just below the bucket without disturbing the measurement of the weight.

The specimen of ~200 mg was measured precisely and placed in the platinum bucket. First the specimen was annealed in $^{16}\text{O}_2$ atmosphere (pressure = 6.7×10^3 Pa) over the temperature range of 300–900°C for 5–8 hrs. The heating rate was 50–100°C/min. In the last 3–6 hrs of annealing, no weight change of the specimen was observed. The specimen was quenched to room temperature and the $^{16}\text{O}_2$ gas was replaced by the $^{18}\text{O}_2$ gas (nominally 99% of ^{18}O). The purity of ^{18}O measured by a mass spectrometer was 98.94%. Then the specimen was reheated to the temperature where the previous annealing was performed. The diffusion annealing lasted 6–24 hrs. In order to follow the diffusion process, the weight increase due to the exchange reaction was monitored continuously.

III. Results and Discussion

3.1 Results and Analysis of Data

Typical weight gain (Δw) for MgO is shown in Fig. 2 as a function of square root of time. The results for NiO were similar to those for MgO. In all the cases, the curve resulted in two straight lines with a transition region between them. If we take an imaginary spherical

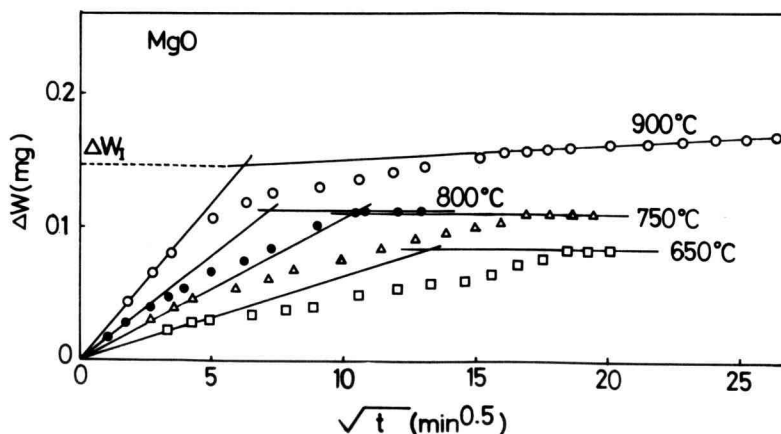


Fig. 2. Some typical weight gains of MgO during the diffusional annealing plotted as a function of \sqrt{t} .

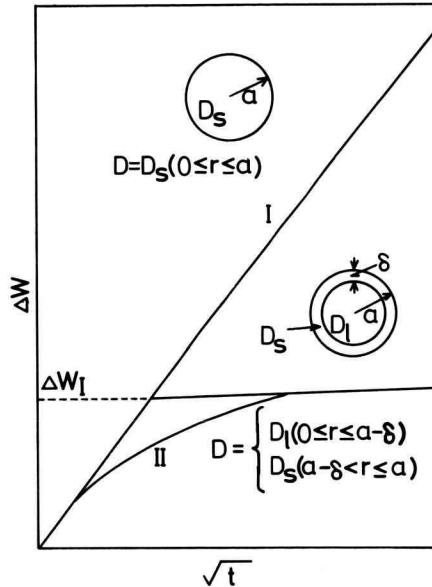


Fig. 3. Model curves of the weight gain (Δw) versus \sqrt{t} for a particle with two different diffusion coefficients.

specimen in which the diffusion coefficient is D_s (surface diffusion coefficient) from $r=0$ to $r=a$ where a is the radius of the sphere, the $\Delta w - \sqrt{t}$ curve will be the line I shown in Fig. 3. However, in the real specimen, the diffusion coefficient is a function of r . To demonstrate the $\Delta w - \sqrt{t}$ curve for the realistic material, we take another spherical specimen in which the diffusion coefficient is D_l (lattice diffusion coefficient) at $0 \leq r \leq a - \delta$ and is D_s at $a - \delta < r \leq a$ where δ is the surface layer thickness ($a \gg \delta$). If we assume that $D_s \gg D_l$, then at the beginning of the diffusion annealing the diffusion distance is very short and $\Delta w - \sqrt{t}$ curve will follow the line I (Fig. 3). As the diffusion distance becomes longer than δ , the $\Delta w - \sqrt{t}$ curve will gradually deviate from the line I. This is the transition region (line II in Fig. 3). Since the surface layer thickness is much smaller than the particle size ($\delta \ll a$), the transition region should appear within the small weight gain of the specimen. When the exchange reaction within the surface layer has been completed, the $\Delta w - \sqrt{t}$ curve will be approximately linear again (plateau or the less steep line). In this region the lattice diffusion (or possibly grain boundary diffusion) is the only diffusion which gives rise to the weight change of the specimen. In the cases of MgO and NiO, the oxygen lattice diffusion is very slow. Consequently, the slope of the second straight line is almost nonexistence.

Some $\Delta w - \sqrt{t}$ curves for Y_2O_3 are shown in Fig. 4 (a). In this oxide the lattice diffusion is relatively fast at temperatures higher than 500°C . Consequently, it is impossible to divide the $\Delta w - \sqrt{t}$ curves at these temperatures into two lines. It is more reasonable to assume that the lattice diffusion is approximately equal to the surface diffusion ($D_{s,0} \sim D_{l,0}$). However, at temperatures lower than 500°C , a curve similar to that for MgO at 900°C was

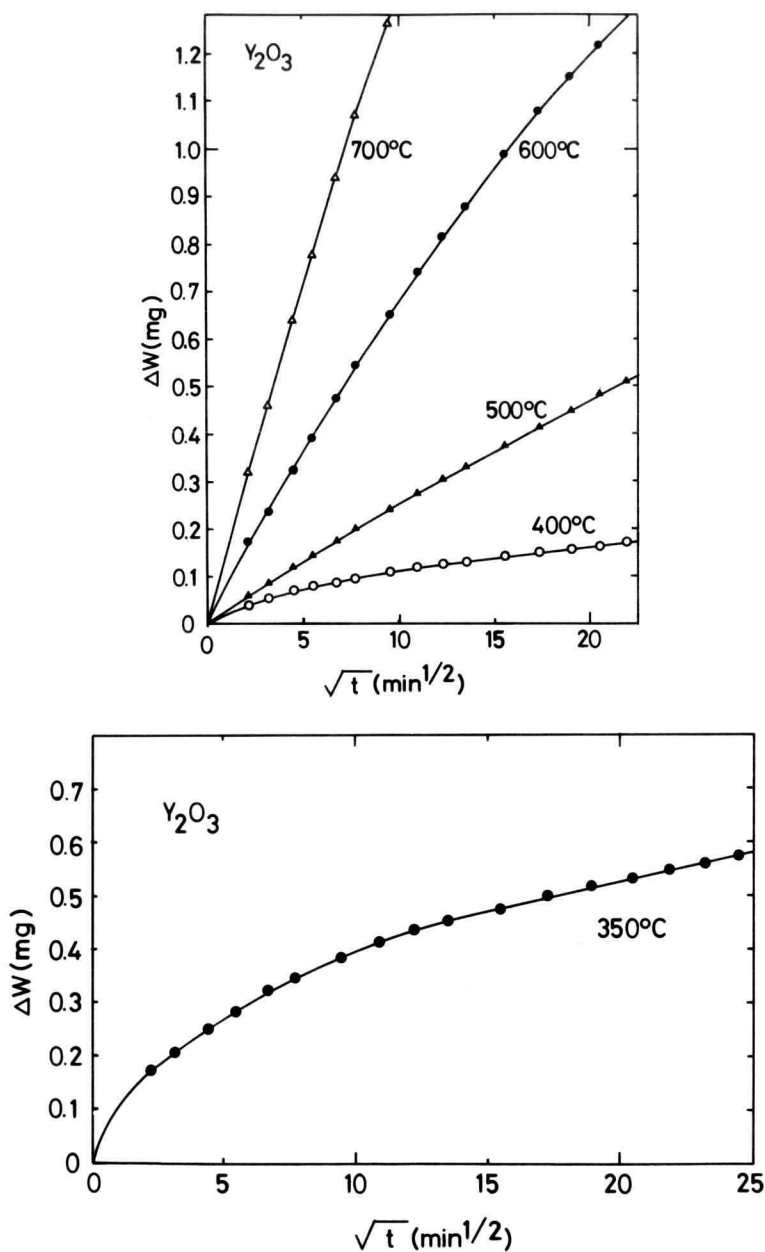


Fig. 4. Some typical weight gains of Y_2O_3 during the diffusional annealing plotted as a function of \sqrt{t} ; (a) 400–700°C, (b) 350°C.

obtained (Fig. 4 (b)). The surface diffusion is obviously higher than lattice diffusion ($D_{s,0} > D_{l,0}$) in this temperature range.

We can calculate the surface diffusion coefficients of three oxides using Eq (2)¹⁵⁾ from the first steep lines of the $\Delta w - \sqrt{t}$ plot except for Y_2O_3 at temperatures higher than 500°C. The

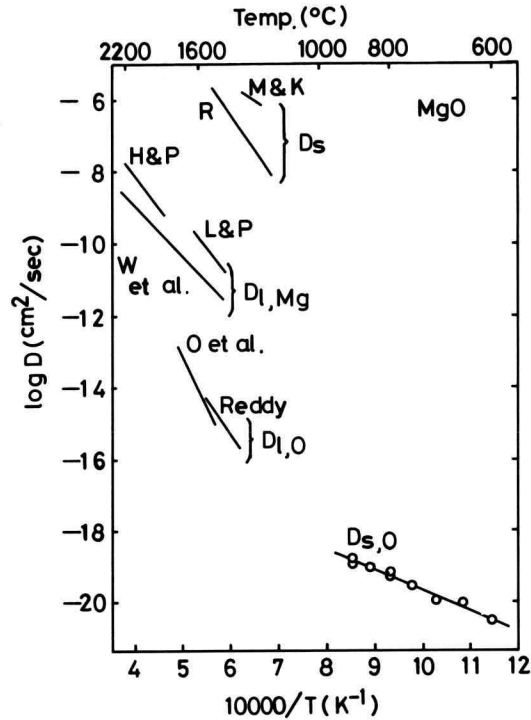


Fig. 5. Surface and lattice diffusion coefficients in MgO.

lattice diffusion coefficient of Y_2O_3 was calculated from the plot at these higher temperatures using Eq (2).

$$\frac{M_t}{M_\infty} = 1 - \sum_{n=1}^{\infty} \frac{6\alpha(\alpha+1) \exp(-D_s q_n^2 t/a^2)}{9+9\alpha+q_n^2 a^2} \quad (2)$$

where M_t is the total amount of ^{18}O in the specimen at time t , M_∞ is the corresponding quantity after infinite time, the q_n 's are the non-zero roots of $\tan q_n = \frac{3q_n}{3+\alpha q_n^2}$, and α is an experimental constant determined by the initial atomic ratio of ^{18}O in the gas phase to ^{18}O in the solid. In the present experiments α was about 1-3.

3.2 MgO

The oxygen surface diffusion coefficients for MgO calculated in this way were plotted in Fig. 5 along with the data (D_s and D_l) obtained by other workers.^{11,16-21} The current result was expressed as

$$D_{s,o} = 9.14 \times 10^{-15} \exp(-107(\text{kJ/mol})/RT) \text{ cm}^2/\text{sec}. \quad (3)$$

The activation energy for the oxygen surface diffusion is in good agreement with the energy (87 kJ/mol) for anion vacancy migration at the {001} surface calculated by Colbourn and Mackrodt.²² Robertson¹⁶) has measured the D_s of MgO bicrystals by thermal grooving. Moriyoshi and Komatsu¹¹) have estimated the surface diffusion coefficient of MgO powder

from the study of combined sintering. In these results the diffusing species (cation or anion) which controls the rate processes is unknown. The lattice diffusion coefficient of Mg in MgO ($D_{l,Mg}$) was studied by Harding and Price,¹⁷⁾ Lindner and Parfitt,¹⁸⁾ and Wuensch *et al.*¹⁹⁾ The lattice diffusion coefficient of oxygen in MgO ($D_{l,o}$) was investigated by Oishi *et al.*²⁰⁾ and Reddy and Cooper.²¹⁾ They are all shown in Fig. 5. It can be noticed that the $D_{s,o}$ of this study is higher than oxygen lattice diffusion coefficients of Oishi *et al.*, and Reddy and Cooper over the temperature range investigated in this study. However, the oxygen surface diffusion coefficient at 1200°C is almost identical with $D_{l,o}$.

The activation energy of oxygen surface diffusion is about 1/4 to 1/5 of the activation energy of oxygen lattice diffusion (370–536 kJ/mol). A similar trend for the activation energies is also observed in the metallic systems.²³⁾

The oxygen surface diffusion coefficient measured in this study is smaller than those obtained by the sintering¹⁾ and the thermal grooving.¹⁶⁾ The explanation to this discrepancy is as follows: Schakelford²⁴⁾ studied the thermal grooving in Al_2O_3 to obtain the surface diffusion coefficient and found that the coefficient obtained in vacuum was similar to that in air²⁵⁾. From this result he concluded that the rate controlling species of the surface diffusion in Al_2O_3 was aluminum (ion) and that oxygen could diffuse through the gas phase. Since the experiments of both Robertson, and Moriyoshi and Komatsu were performed in air, the oxygen could diffuse through the gas phase. Then it is more probable that the cation surface diffusion coefficient has been determined in their studies. The difference between the cation surface diffusion coefficient obtained from these methods and the anion surface diffusion

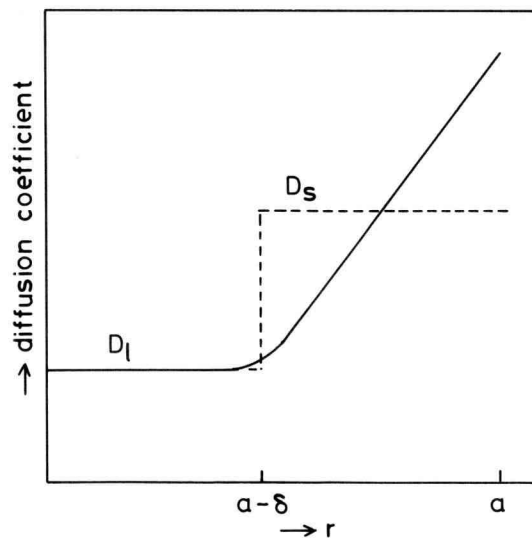


Fig. 6. A profile of the diffusion coefficient in a spherical model which represents a realistic material. In the present study we assumed that the diffusion coefficient near the surface layer is represented by the dotted line.

coefficient measured in this study agrees qualitatively with the relative difference between cation lattice and anion lattice diffusion coefficients, i.e., in both cases the diffusion of the cation is faster than the anion. Another important difference in the results of these methods is that the diffusion processes which were observed by Robertson, and Moriyoshi and Komatsu are probably the diffusion along the surface, whereas the diffusion in this study is, by the nature of investigation, diffusion through the surface layer. It is generally expected that the diffusion coefficient in the surface layer is a function of radius, r . As shown in Fig. 6, the diffusion coefficient is very high at $r=a$ (surface). As the r decreases, the diffusion coefficient decreases gradually to the value in the bulk and finally at $r \leq a - \delta$ the diffusion coefficient is equal to the lattice diffusion coefficient. However, for mathematical simplicity, we assume that within the surface layer of the thickness δ , the property of material is homogeneous and that a diffusion coefficient D_s which is actually the average of varying diffusion coefficients is constant within the surface layer. Consequently, it is not surprising to find that the D_s obtained in this study is closer to the lattice diffusion coefficient than the value measured by other methods.

From the less steep line at 900°C in Fig. 2, a diffusion coefficient (presumably the oxygen lattice diffusion coefficient) can be calculated. It is 2.2×10^{-22} cm²/sec which is approxi-

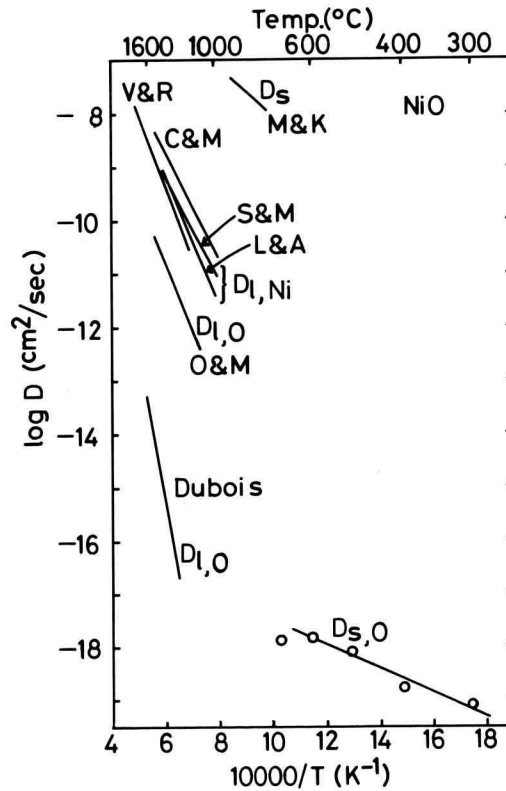


Fig. 7. Surface and lattice diffusion coefficients in NiO.

mately on the line extended from the results of Oishi *et al.*²⁰⁾ and Reddy and Cooper²¹⁾ (Fig. 5).

3.3 NiO

In Fig. 7 the effect of temperature on the $D_{s,0}$ of NiO is shown. From the least square method, the $D_{s,0}$ is expressed by

$$D_{s,0} = 5.04 \times 10^{-16} \exp(-42.7(\text{kJ/mol})/RT) \text{ cm}^2/\text{sec}. \quad (4)$$

The value of $D_{s,0}$ at 700°C was not included in the calculation of Eq. (4) because the evaporation of NiO began slightly at 700°C, i.e., the slope of the first steep line in the $\Delta w - \sqrt{t}$ plot at 700°C was almost identical with that at 600°C.^{13),14)} The evaporation of NiO was more pronounced at 800°C where the condensation of NiO on the thermocouple tube and quartz glass was observed.

The surface diffusion coefficient obtained in this study was compared in Fig. 7 with the results of other studies.^{1),26)-28)} It is clear that the surface diffusion coefficient obtained from a sintering study¹⁾ is about 9 orders of magnitude higher than the current results. In the sintering study δ was assumed to be equal to 0.1 nm and independent of temperature. However, as will be shown later, δ ranges from 0.3–3.0 nm and depends upon the temperature. If we take into account this fact, the difference between the results of these two methods will be about 7–8 orders of magnitude. The discussion given for the surface diffusion of MgO can be extended to explain the discrepancy in the surface diffusion coefficient of NiO. If we assume that the surface diffusion coefficient determined by the study of sintering is for cation (Ni^{2+}), the surface and lattice diffusion coefficients of cation are higher than those of anion. The difference in diffusion direction (along the surface or through the surface layer) may also account, in part, for the discrepancy in Fig. 7. In contrast, the activation energy of D_s (87.0 kJ/mol which is actually $Q_\delta + Q_s$) obtained from the sintering is nearly equal to the current results (i.e., $Q = Q_\delta + Q_s = 29.4 + 42.7 = 72.1$ kJ/mol).

The oxygen grain boundary diffusion coefficient, $D_{b,0}$, for NiO was calculated from the second slow line in the $\Delta w - \sqrt{t}$ plot using the procedure described elsewhere.¹⁴⁾ It was 3.1×10^{-18} cm²/sec at 700°C which was almost equal to the expected oxygen surface diffusion coefficient of NiO (2.6×10^{-18} cm²/sec) at this temperature.

3.4 Y₂O₃

The oxygen surface diffusion coefficients for Y₂O₃ in the temperature range 300–450°C are shown in Fig. 8 (open circles and squares). Also shown in Fig. 8 are the oxygen lattice diffusion coefficient (closed circles and triangles). A least squares fit to these data leads to

$$D_{s,0} = 2.40 \times 10^{-10} \exp(-76.6(\text{kJ/mol})/RT) \text{ cm}^2/\text{sec}. \quad (5)$$

and

$$D_{l,0} = 1.42 \times 10^{-9} \exp(-125(\text{kJ/mol})/RT) \text{ cm}^2/\text{sec}. \quad (6)$$

The $D_{s,0}$ is about two to three orders of magnitude higher than the $D_{l,0}$. The diffusion coefficients for Y₂O₃ reported in the literature^{29),30)} are shown in the figure. The oxygen lattice diffusion coefficients obtained in this study are in good agreement with those of the

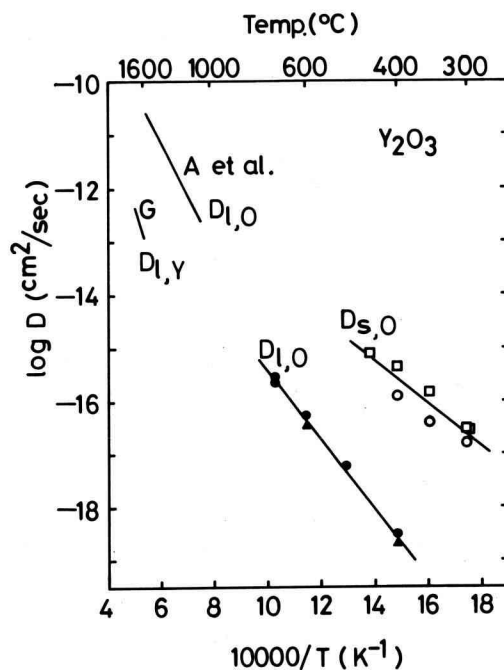


Fig. 8. Surface and lattice diffusion coefficients in Y_2O_3 .

literature. The lower activation energy of $D_{l,o}$ in this study might be the indication of the extrinsic region. However, more experiments are needed to confirm this.

3.5 Surface Layer Thickness

If we assume that the exchange reaction in the surface layer has been completed at the intersection of two lines (Fig. 2), the surface layer thickness for a compound $M_\alpha O_\beta$ can be estimated by substituting the weight change*, Δw_1 , at the intersection into the following equation:

$$\delta = a \left\{ 1 - \left(1 - \frac{\Delta w_\delta M_{M_\alpha O_\beta}}{2\beta w f} \right)^{1/3} \right\} \quad (7)$$

where w is the weight of specimen, $M_{M_\alpha O_\beta}$ is the formula weight of $M_\alpha O_\beta$, and f is a constant determined by the experimental condition. In the present experiment the value of f is approximately equal to unity. Eq. (7) was derived under the assumption that a spherical specimen with radius a has the surface layer thickness of δ .

The values of δ obtained from Eq. (7) are shown in Fig. 9. They can be represented by

* Actually the exchange reaction is taking place also before the specimen was heated to the experimental temperature. The weight gain during this period is added to Δw_1 . Therefore, the weight gain shown in Fig. 2 is the part of the weight gain (Δw_δ) which was used to calculate δ .

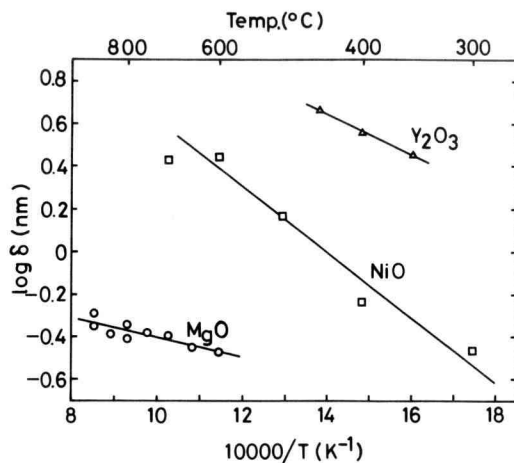


Fig. 9. Surface layer thicknesses of oxides measured by isotope exchange reaction.

Table 1 Comparison of surface layer thicknesses in oxides.

Oxides	Temperature (°C)	Surface layer thickness (nm)	Temperature dependence (kJ/mol)	Method of measurement
CoO	253-723	4.0-60	54	kinetic ^{7,9)}
Cu ₂ O	280-380	7.5-92	109	kinetic ³¹⁾
TiO ₂ (rutile)	883-965	4.5-20	130	kinetic ⁸⁾
α-Al ₂ O ₃	900-1000	3.0-13	176	kinetic ³¹⁾
NiO	300-600	0.3-2.8	29	isotope exchange
Y ₂ O ₃	350-450	2.8-4.6	18	isotope exchange
MgO	600-900	0.3-0.5	8.8	isotope exchange

$$\delta = 1.14 \exp(-8.8(\text{kJ/mol})/RT) \text{ nm}$$

$$\delta = 1.42 \times 10^2 \exp(-29.4(\text{kJ/mol})/RT) \text{ nm}$$

$$\delta = 9.00 \times 10^1 \exp(-18.0(\text{kJ/mol})/RT) \text{ nm}$$

and

for MgO, NiO, and Y₂O₃, respectively.

It can be noticed that among the surface layer thicknesses obtained by the isotope exchange reaction, the δ of MgO is the smallest. Additional experiments are needed to find the cause of this difference. In Table 1 are shown the surface layer thicknesses obtained by both the kinetic method and the isotope exchange reactions. Admittedly there is insufficient amount of data. Especially the measurements of the δ in one oxide using both methods are needed. However, there is a general trend that the surface layer thicknesses obtained by the kinetic method are much larger than those obtained by the isotope exchange reaction. The difference is partially due to the fact that in the kinetic method the surface layer thickness is measured during the formation of product layer which has a disturbed structure.¹⁰⁾⁻¹²⁾ Consequently, the kinetic method gives thicker surface layer.

Since the surface layer thickness of MgO measured in this study is 0.3-0.5 nm (lattice

parameter of MgO is ~ 0.4 nm), there might be some concern about the nature of the oxygen ions which have been exchanged with ^{18}O , i.e., most of the weight change could be caused by the oxygen which has been chemisorbed on the surface of MgO. To test this possibility, specimen was first annealed at 650°C in an oxygen pressure of 1.3×10^2 Pa. After reaching an apparent equilibrium, the oxygen pressure was increased to 7.3×10^3 Pa and then the weight gain due to the chemisorption was measured. From the measurement, it was found that the weight change of 0.01 mg during the oxygen isotope exchange reaction is caused by oxygen which is chemisorbed on the surface of MgO. This experiment suggests that $\sim 4\%$ of oxygen which has been exchanged with ^{18}O were the chemisorbed oxygen.

IV. Conclusions

The oxygen surface diffusion coefficients and the surface layer thicknesses in MgO, NiO, and Y_2O_3 have been determined by recording the weight of oxides during the ^{18}O -exchange reaction between $^{18}\text{O}_2$ gas and oxide powder using a microbalance. The surface diffusion coefficients of oxygen can be represented by

$$D_{s,0} = 9.14 \times 10^{-15} \exp(-107(\text{kJ/mol})/\text{RT}) \text{ cm}^2/\text{sec}$$

$$D_{s,0} = 5.04 \times 10^{-16} \exp(-42.7(\text{kJ/mol})/\text{RT}) \text{ cm}^2/\text{sec}$$

and $D_{s,0} = 2.40 \times 10^{-10} \exp(-76.6(\text{kJ/mol})/\text{RT}) \text{ cm}^2/\text{sec}$
for MgO, NiO, and Y_2O_3 , respectively.

The oxygen surface diffusion measured by the current method is diffusion through a surface layer rather than diffusion along a surface. This can be one of the reasons why the surface diffusion coefficients (MgO and NiO) obtained by other methods (thermal grooving and sintering) are higher than the current results. Another possible reason was also discussed.

The surface layer thicknesses obtained by the oxygen isotope exchange reaction are in general smaller than those determined by the kinetic method.

Acknowledgements

The authors wish to thank H. Takamura, Y. Hirabayashi, and R. Sanosaka for obtaining some of the data. This study was supported in part by the Science Foundation of the Ministry of Education.

References

- 1) Y. Moriyoshi and W. Komatsu, *Yogyo-Kyokai-Shi*, **81**, 102-107 (1973).
- 2) K. Hirota and W. Komatsu, *J. Am. Ceram. Soc.*, **60**, 105-107 (1977).
- 3) W.W. Mullins, *J. Appl. Phys.*, **28**, 333-339 (1957).
- 4) W.W. Mullins, *Trans. Metal. AIME*, **218**, 354-61 (1960).
- 5) R.T. King and W.W. Mullins, *Acta Met.*, **10**, 601-606 (1962).
- 6) F.A. Nichols and W.W. Mullins, *J. Appl. Phys.*, **36**, 1826-35 (1965).

- 7) T. Maruyama, K. Takada, and W. Komatsu, *Z. Physik. Chem. NF*, **102**, 221-30 (1976).
- 8) M. Yamashita, T. Maruyama, and W. Komatsu, *ibid*, **105**, 187-196 (1977).
- 9) W. Komatsu, Y. Chida, and T. Maruyama, in 'Reactivity of Solids', eds. K. Dyrek, J. Haber, and J. Nowotny, Elsevier Scientific, Amsterdam, p. 430-435 (1982).
- 10) W. Jander and K.F. Weitendorf, *Z. Elektrochem. angew. phys. Chem.*, **41**, 435-444 (1935).
- 11) G.F. Hüttig, *ibid*, **41**, 527-538 (1935).
- 12) C. Kröger, G. Ziegler, *Glastech. Ber.*, **26**, 346-353 (1953); *ibid*, **27**, 199-212 (1954).
- 13) W. Komatsu, Y. Ikuma, K. Uematsu, Y. Kawashima, S. Yamaguchi, and H. Takamura, in 'Ceramic Powders', ed. P. Vincenzini, Elsevier Scientific, Amsterdam, p. 699-704 (1983).
- 14) W. Komatsu and Y. Ikuma, *Z. Physik. Chem. NF*, **131**, 79-88 (1982).
- 15) J. Crank, 'Mathematics of Diffusion', p. 88, Oxford (1956).
- 16) W.M. Robertson, in 'Sintering and Related Phenomena', eds. G. C. Kuczynski et al., Gordon and Breach, New York, p. 215-32 (1967).
- 17) B.C. Harding and D.M. Price, *Philos. Mag.*, **26**, 253-60 (1972).
- 18) R. Lindner and G.D. Parfitt, *J. Chem. Phys.*, **26**, 182-185 (1957).
- 19) B.J. Wuensch, W.C. Steele, and T. Vasilos, *ibid*, **58**, 5258-66 (1973).
- 20) Y. Oishi, K. Ando, H. Kurokawa, and Y. Hiro, *J. Am. Ceram. Soc.*, **66**, c60-62 (1983).
- 21) K.P.R. Reddy and A.R. Cooper, *ibid.*, **66**, 664 (1983).
- 22) E.A. Colbourn and W.C. Mackrodt, presented at the conference on Structure-Property Relations for MgO/Al₂O₃ at MIT, June (1983).
- 23) J.H. Brophy, R.M. Rose, and J. Wulff, 'Thermodynamics of Structure', John Wiley, New York (1964).
- 24) J.F. Shackelford and W. Scott, *J. Am. Ceram. Soc.*, **51**, 688-92 (1968).
- 25) W.M. Robertson and R. Chang, *Mater. Sci. Res.*, **3**, 49-60, eds W.W. Kriegel and H. Palmour, III, Plenum Publishing Co., New York (1966).
- 26) R. Lindner and A. Akerstrom, *Disc. Faraday Soc.*, **23**, 133 (1957); M.T. Shim and W.J. Moore, *J. Chem. Phys.*, **26**, 802 (1957); J.S. Choi and W.J. Moore, *J. Phys. Chem.*, **66**, 1308 (1962); M.L. Volpe and J. Reddy, *J. Chem. Phys.*, **53**, 1117 (1970).
- 27) M. O'Keeffe and W.J. Moore, *J. Phys. Chem.*, **65**, 1438 (1961); *ibid*, **65**, 2277 (1961).
- 28) C. Dubois, C. Monty, and J. Philibert, *Philos. Mag.*, **46**, 419 (1982).
- 29) K. Ando, Y. Oishi, H. Hase, and K. Kitazawa, *J. Am. Ceram. Soc.*, in press.
- 30) R.J. Gaboriaud, *J. Solid State Chem.*, **35**, 252-261 (1980).
- 31) T. Maruyama and W. Komatsu, unpublished work.